

INVESTIGATION OF THE STRUCTURE OF RAPIDLY QUENCHED Fe-Sn-Si-B SYSTEMS WITH VARYING Si/B CONTENT

E. G. Çoker¹, I. Janotova¹, P. Svec¹, I. Matko¹, D. Janickovic¹, U. Topal², P. Svec Sr.¹

¹*Institute of Physics, Slovak Academy of Sciences, Bratislava, Slovakia*

²*UME Tubitak, Gebze, Turkey*

Email: eylemcoker@hotmail.com

Received 15 May 2017; accepted 25 May 2017

1. Introduction

The amorphous alloys have many bases, Fe-B based alloys are the best representatives of the classical metallic glass systems which have many applications according to the soft magnetic characteristics. They have been a wide research area for decades in the world because of their physical properties and structures [1]. The investigations were based on the addition of a variety of elements into the Fe-B based alloys [2]. The consequence of this effort was the finding of formation of nanocrystalline phase by restrained crystallization of Fe-B based amorphous alloys which was related to Fe-Si-B systems [3]. These systems composed in the basis of other systems are explained in the phase of literature briefly, there are three binaries in the Fe-Si-Sn ternary system which are Fe-Sn, Fe-Si and Si-Sn systems [4].

The equilibrium phase diagram of the Fe-Sn system has been researched by many authors [5–9]. Thermodynamic characterization by Nüssler et al. [5] included two metastable phases Fe₃Sn and Fe_{0.565}Sn_{0.435} [5, 9], while the stable Fe₅Sn₃ phase was omitted. Kumar et al. [6] thermodynamically modelled this system and thermodynamic descriptions recently reported by Huang et al. [8]. The equilibrium phases included in this system are: liquid, α -Fe, γ -Fe, (Sn) and four intermetallic compounds: Fe₅Sn₃, Fe₃Sn₂, FeSn, and FeSn₂.

The Fe-Si binary system thermodynamically appraised by Lacaze and Sundman [4,10] has been widely recognized in literature [11–14]. The solution phases are given as: liquid, (γ -Fe) and (α -Fe). The bcc-solid solution has two forms, disordered α -Fe (A2) and ordered α 1 (B2) and α 2 (D03). Silicon versus iron content is very low so we do not have those compositions. Five intermetallic compounds occurs in the Fe-Si binary system: Fe₂Si, Fe₅Si₃, FeSi, FeSi₂-H and FeSi₂-L but they aren't observed in rapidly quenched Fe-Si systems.

The Si-Sn binary system [4, 15] exhibits a eutectic reaction at 605 K. The eutectic point is very close to the melting point of pure Sn. Under normal pressure, the stable phases are: liquid, the (Si) solid solution and the (Sn) solid solution. No binary compound exists in this system. From the above three binary systems, only the Fe-Sn system has the ability to interfere gap characterizing formation of the immiscible alloy, for that reason much more attention should be paid to the role of Si on the solidification of Fe-Sn based alloy.

Those phases have importance in understanding the soft magnetic materials behaviours. The effects of adding various elements can be found in literature but a few results have been published for rapidly quenched Fe-Sn-B ribbons for the fact that Sn element just dissolves in the solid Fe(Sn) and forms no solid dispersion with boron [16,17]. This can be under the assumption of negatively affect glass forming talent of any Fe-Sn-B alloy. However, the effect of Sn addition can be investigated by many reasons such as atomic radius misfit, low melting temperature and representing a Mössbauer active element implementing the technique for microstructural analysis [18].

In this study, the different rapidly quenched compositions of Fe-Sn-Si-B were investigated by means of the microstructure and morphology of the phases formed upon

thermally activated crystallization. The measurements were taken from X-ray diffraction, transmission electron microscopy and differential scanning calorimetry.

2. Experimental Details

Amorphous ribbons with thickness around 20-30 μ m and width of 6 mm were prepared by planar flow casting from master alloys with variable chemical compositions (purity of the components were better than 99.9%). Casting of ribbons performed after induction melting of the master alloys to casting temperatures about 200 K higher than the alloy melting point. The planar flow casting temperature was from 1473 K to 1523 K variably and for all the samples there was a waiting time for 1 min at 1373 K before heating to the final casting temperature. The composition of the prepared samples with the results from differential scanning calorimetry are in Table 1. The amorphous state after rapid quenching was checked by X-ray diffraction analysis (XRD) in Bragg–Brentano geometry using Bruker D8 Advance diffractometer (Cu K α radiation). Samples were polished by ion-beam milling using a Gatan PIPS machine. The microstructure and morphology of the crystallized products were analysed by transmission electron microscopy (TEM) using JEOL JEM-2000FX electron microscope.

Ribbons were weighed and prepared for the thermal measurements in differential scanning calorimetry (DSC, Perkin–Elmer DSC7). The thermal regime was given in five steps. The first step was heating from 300 K to 873 K with heating rate 10K/min. Then cooling from 873 K to 300 K was performed at a rate of 40 K/min. The sample was held for 5 minutes at 300 K for stabilization, then the first and the second steps were repeated, respectively, to obtain the proper baseline-subtracted DSC signal.

3. Results and Discussions

The rapidly quenched as-cast ribbons have been examined by X-ray diffraction, TEM and DSC for the morphology, structure and crystallization temperatures.

The XRD patterns of the analysed samples (Fig. 1) suggest that the Sn+Si at.% content is important for glass forming ability of the system. Considering the content of alloying elements, when the addition of Sn+Si is higher than 9 at.% then the content of quenched-in crystallinity begins to be seen more at the expense of the amorphous phase. We can add to this assumption the boron content also: if the boron content is less than 10 at.% then again the crystallisation begins to occur. The amorphous matrix is seen in the XRD patterns in the curves which are Fe₈₁Sn₇B₁₂-Fe₈₁Sn₇Si₂B₁₀-Fe₈₃Sn₅Si₂B₁₀, thus for ribbons where the boron content is greater/equal 10 at.% and Sn+Si content is at most 9 at.%.

The results from thermal analyses of the examined compositions are presented in Table 1. The expected intervals of formation of crystalline phases from amorphous state were obtained by DSC (Fig. 2). In the first step of transformation the formation of α -Fe was observed in amorphous matrix which can be also seen in XRD curves from as-quenched samples and in the second transformation step the formation of borides, which generally deteriorate soft magnetic properties, was seen. The temperatures of the crystallization onsets given by $T_{x(1)}$ and $T_{x(2)}$ values are changing with the ratio of addition of Fe-Sn/Si-B. The difference between the temperatures of the maximum crystallization rates $T_{max(1)}$ and $T_{max(2)}$ indicates the stability of the remaining amorphous matrix.

TEM analysis of the investigated systems in as-quenched state shown in Fig. 3 confirms the hypothesis about the glass formability proposed above. Analysis of images shows that different but relatively small amounts of quenched-in nanocrystalline grains with dimensions around 20 – 40 nm are present in the amorphous matrix, which transforms to α -Fe upon heating, as shown in DSC traces in Fig. 2.

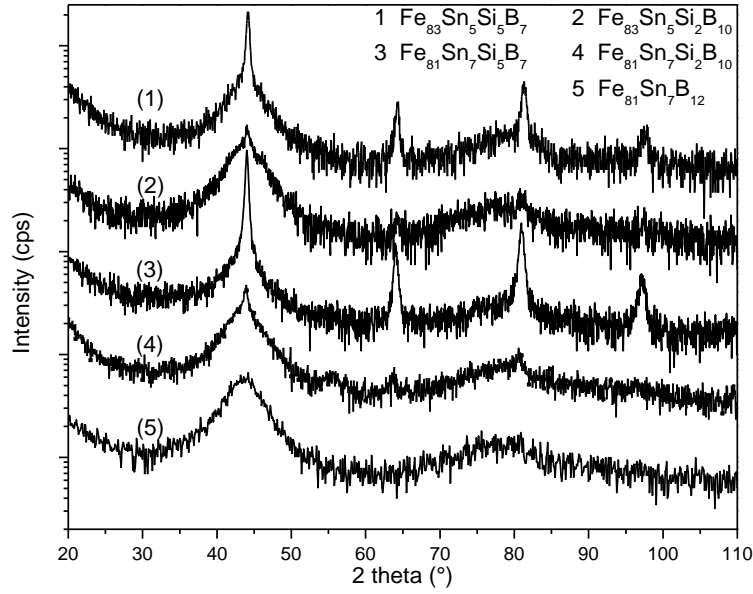


Fig.1: XRD diffraction patterns of the ribbons in as-quenched state.

Tab.1. Results from DSC: the temperatures of the crystallizations onset are given by $T_{x(1,2)}$, the temperatures of the maximum crystallization rate are given by $T_{max(1,2)}$.

Composition	T_{x1} (K) ± 0.2	T_{max1} (K) ± 0.2	T_{x2} (K) ± 0.2	T_{max2} (K) ± 0.2	$T_{max2}-T_{max1}$ (K)
$Fe_{81}Sn_7Si_2B_{10}$	652.8 K	670.4 K	794.5 K	800.8 K	130,4 K
$Fe_{81}Sn_7Si_5B_7$	644.9 K	658.6 K	791.9 K	799.2 K	140,6 K
$Fe_{83}Sn_5Si_2B_{10}$	643.4 K	667.6 K	775.1 K	780.8 K	113,2 K
$Fe_{83}Sn_5Si_5B_7$	605.8 K	641.4 K	789.5 K	795.7 K	154,3 K
$Fe_{81}Sn_7B_{12}$	653.7 K	667.4 K	758.9 K	764.6 K	97.2 K

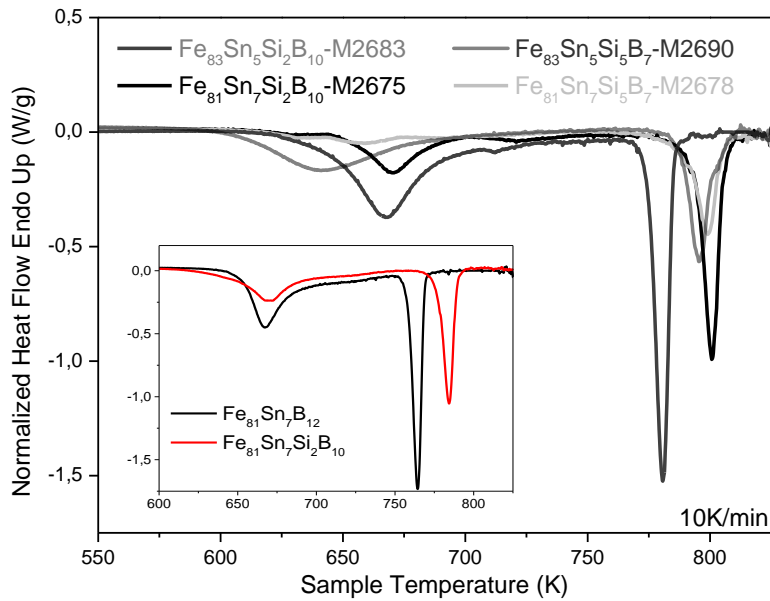


Fig.2: DSC curves of as-quenched ribbons based on Fe-Sn-B with and without addition of silicon.

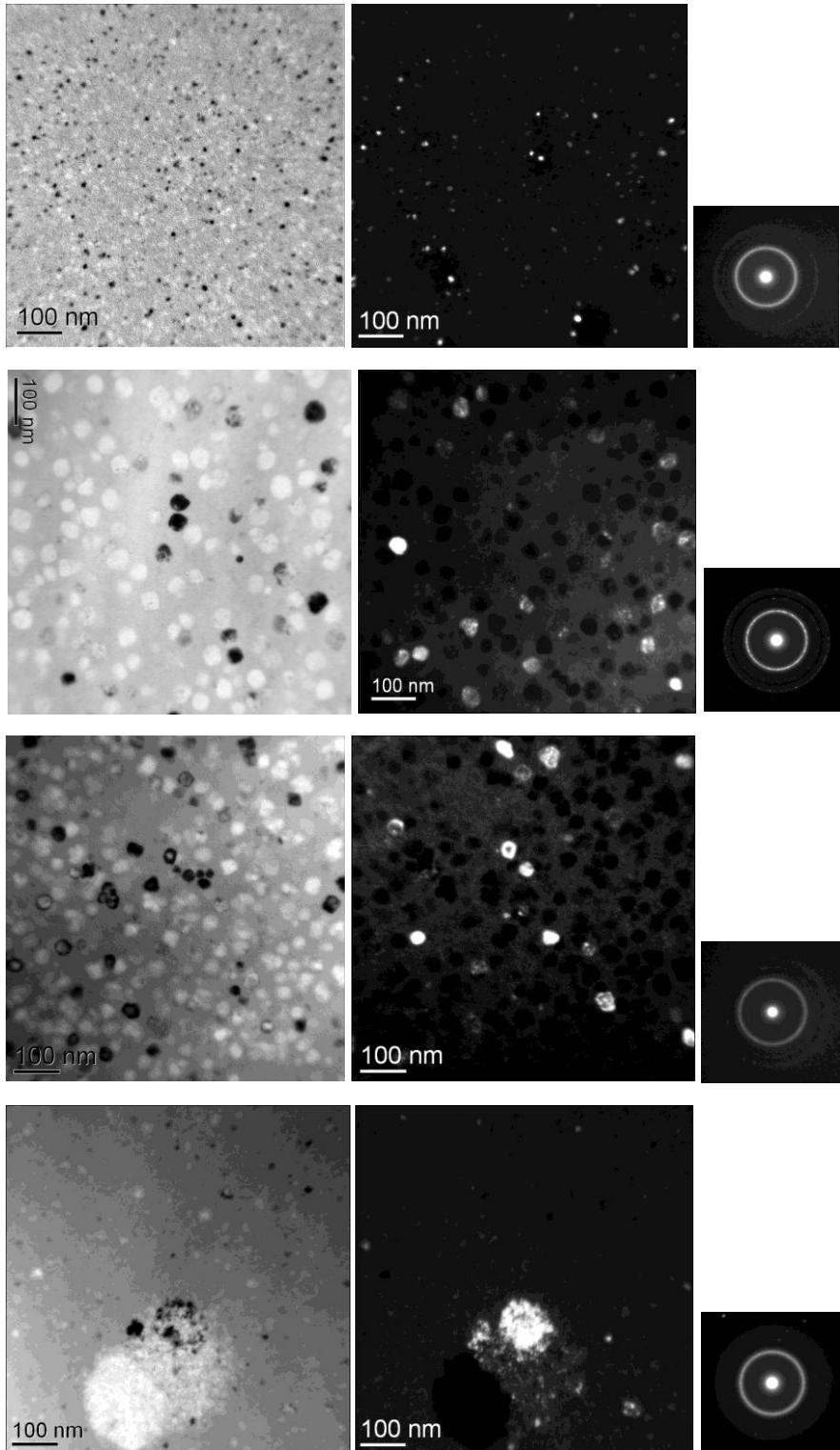


Fig.3: Bright and dark field TEM images and electron diffraction patterns of the $Fe_{81}Sn_7Si_2B_{10}$, $Fe_{81}Sn_7Si_5B_7$, $Fe_{83}Sn_5Si_2B_{10}$, $Fe_{83}Sn_5Si_5B_7$ ribbons in as-quenched state, respectively.

4. Conclusions

Possibility of preparation and qualitative glass formability have been studied on selected alloys of the investigated Fe-Sn-Si-B rapidly quenched system. Preliminary

orientational criterion for glass formation in this system has been proposed on the basis of total content of alloying elements (Sn+Si) and the content of metalloid (boron). Experimental results from structure analysis by X-ray diffraction, TEM and electron diffraction are in accord with the proposed criterion. The size of the as-quenched α -Fe nanocrystals which is 20 – 40 nm allows to assume that controlled nanocrystallization during the first transformation stage will lead to sufficient population of nanocrystalline grains embedded in remaining amorphous matrix to yield a soft magnetic material with potentially interesting properties, warranting further investigation of the Fe-Sn-Si-B system.

Acknowledgement

This work was supported by the project CEKOMAT I, ITMS 26240120006 from the Research and Development Operational Program funded by the ERDF.

References

- [1] A.L. Greer, *Acta Metall.* **30** (1982) 171.
- [2] E. Illekova, I. Mat'ko, P. Duhaj, F.-A. Kuhnast, *J. Mater. Sci.* **32** (1997) 4645.
- [3] Y. Yoshizawa, S. Oguma, K. Yamaguchi, *J. Appl. Phys.* **64** (1988) 6044.
- [4] X. Wanga,b, B. Zhoua, Z.Guoa, Y. Liua, J. Wanga, X. Sub.c, Experimental investigation and thermodynamic calculation of the Fe–Si–Sn system, *Calphad* **57** (2017) 88-97.
- [5] H. Nüssler, O. Von Goldbeck, P. Spencer, A thermodynamic assessment of the iron–tin system, *Calphad* **3** (1979) 19–26.
- [6] K.H. Kumar, P. Wollants, L. Delaey, Thermodynamic evaluation of Fe–Sn phase diagram, *Calphad* **20** (1996) 139–149.
- [7] H. Okamoto, T.B. Massalski (Ed.)^{2nd} ed. Binary Alloy Phase Diagrams 2, ASM Int,
- [8] Y.C. Huang, W. Gierlotka, S.W. Chen, Sn–Bi–Fe thermodynamic modeling and Sn–Bi/Fe interfacial reactions, *Intermetallics* **18** (2010) 984–991.
- [9] H. Okamoto, Fe–Sn (Iron–Tin), Binary Phase Diagrams Updating Service, Errata, 1991.
- [10] J. Lacaze, B. Sundman, An assessment of the Fe–C–Si system, *Metall. Trans. A* **22** (1991) 2211–2223.
- [11] C. Sha, S. Liu, Y. Du, H. Xu, L. Zhang, Y. Liu, Experimental investigation and thermodynamic reassessment of the Fe–Si–Zn system, *Calphad* **34** (2010), 405–414.
- [12] M.G. Poletti, L. Battezzati, Assessment of the ternary Fe–Si–B phase diagram, *Calphad* **43** (2013) 40–47.
- [13] H.M. Henaio, A. Sugiyama, K. Nogita, Comparison of solidification behavior between in situ observation and simulation of Fe–C–Si system, *J. Alloy. Compd.* **613** (2014) 132–138.
- [14] W. Zheng, X.G. Lu, Y. He, Y. Cui, L. Li, Thermodynamic assessment of the Fe–Mn–Si system and atomic mobility of its fcc phase, *J. Alloy. Compd.* **632** (2015) 661–675.
- [15] R. Olesinski, G. Abbaschian, The Si–Sn (silicon–tin) system, *J. Phase Equilib.* **5** (1984) 273–276.
- [16] R.A. Dunlap, *Solid State Commun.* **43** (1982) 57.
- [17] H. Okamoto, Phase Diagrams of Binary Iron Alloys, ASM International, Materials Park, 1993. 131-137.
- [18] M. Miglierini, V. S. Rusakov, AIP Conf. Proc. 1258 (2010) 29, <http://dx.doi.org/10.1063/1.3473896>.